

Expansion Sequences and their Clusters of the All Space-filling Periodic Polyhedral Honeycombs

Robert C. Meurant

Director, Institute of Traditional Studies • 4/1108 Shin-Seung Apt, ShinGok-Dong 685 Bungi, Uijeongbu-Si, Gyeonggi-Do, Republic of Korea 480-070 • Email: rmeurant@gmail.com

Abstract

In previous research, I classify the proper honeycombs into three symmetry groups, identify the component polytopes of *GE* polyhedra, *PP* polytopes, and *NE* polytopes, and advance a schema that adequately represents the relationship between the *GEs* and *PPs* and their corresponding honeycombs [1, 2]. Herein, I describe the expansion sequences that relate honeycomb to honeycomb, and identify the clusters of sequences that they form. At each step of these sequences, the lattice cell dimension increases by unit length of the edge length of the polyhedra. These sequences are characterized by complementary sets of *PPs* separating, or morphing by turn, while their respective *NEs* project (stretch), or expand, respectively, by turn. I find that just four morphing transformations characterize each of these sequences: $VT \rightarrow CB$, $OH \rightarrow SR$, $CO \rightarrow TC$, and $TO \rightarrow GR$. The formal order can be generalized to the tessellations of the plane, and suggests a refinement of my earlier metaorder of polyhedra (and tessellations) to accommodate the *VT* polytope, and recognize the common patterns of alternating separation and expansion of faces that rigorously relate the 3D polyhedra and 2D tessellations for all 5 symmetry classes. The geometry of the sequences and clusters described suggest diverse applications, including deployable space structures, transfer interfaces, tissue engineering, new materials, metamaterials, sensors, solar cells, battery electrodes, and filters.

Keywords: polyhedra, honeycomb, array, tessellation, structural morphology, spatial harmony, form, order, all-space-filling.

This paper substantially expands my earlier paper “*Sequences of the All Space-filling Periodic Polyhedral Honeycombs*”, published in L. Li et al. (eds.), Proceedings of *The Eighth International Conference on Information*, Tokyo, May 17–18, 2017 [3].

Contribution

- Expansion sequences and clusters of the All Space-filing honeycombs are identified.
- Their expansion characteristics are described as alternating separation and morphing of pairs of *PPs*, accompanied by projection and expansion of their respective *NEs*.
- The four key morphs of the sequence steps are identified and described.
- The honeycomb order is extended to the regular & semi-regular planar tessellations.
- A revision of the author’s metaorder of the polyhedra and tessellations is suggested.

Glossary

- GE* : The 4 Great Enablers, of +/- orientation Tetrahedron T^+, T^- , or truncated tetrahedron, D^+, D^- .
- PP* : The 8 Primary Polytopes: VerTex *VT*, CuBe *CB*, Truncated Octahedron *TO*, Great Rhombic cuboctahedron *GR*, OctaHedron *OH*, CubOctahedron *CO*, Truncated Cube *TC*, and Small Rhombic octahedron *SR*.
- NE* : The 10 Neutral Elements: the Diagonal Edge *DE* (i.e., $\sqrt{2}$), (2D) Neutral Vertex *NV*, (transverse) Square *SQ*, Rotated Square *RS*, and OctaGon *OG*, and their respective prisms, the Diagonal Prism *DP* (axial square), Axial Edge *AE*, Square Prism *SP* (neutral cube), Rotated Prism *RP* (rotated cube), and Octagonal Prism *OP*.
- RCL* : Reference Cubic Lattice, RCL_1 and RCL_2 , each with nodes at the centers of the other's cubes.
- RTL* : Reference Tetrahedral Lattice, there being two for each *RCL*: RTL_1^α and RTL_1^β , RTL_2^α and RTL_2^β .
- V3* : $\sqrt{3}$ axial Vertex "face" of *VT*, *CB*, or *T*. *V4* : $\sqrt{1}$ axial Vertex "face" of *VT*
- TR* : $\sqrt{3}$ axial Triangular face, +ve (upper Δ) TR^+ of *OH*, *SR*, or *D*; -ve (up. ∇) TR^- of *TC*, *CO*, or *T*.
- HG* : $\sqrt{3}$ axial Hexagonal face, of *TO*, *GR*, or *D*.

1. Introduction: Symmetry Classes of the All Space-filing Periodic Polyhedral Arrays

In previous research [1, 2], I establish that the all-space-filling periodic polyhedral honeycombs exhibit three symmetry classes of Class I: $\{2,3,3|2,3,3\}$, Class II: $\{2,3,3|2,3,4\}$, and Class III: $\{2,3,4|2,3,4\}$. Instead of considering the various component polyhedra as being of equivalent worth, I investigate their qualitative diversity. They form distinct sets that play different roles in the overall honeycomb; and different polyhedra play similar roles in different honeycombs, in a highly regular manner. I identify the polytope components of these honeycombs as being the 4 Great Enablers (*GEs*): (T^+, T^-, D^+, D^-) ; 8 Primary Polytopes (*PPs*) in two distinct sets of (VT, CB, TO, GR) , which can self-reflexively form honeycombs, and (OH, CO, TC, SR) , which do not; and Neutral Elements (*NEs*): (DE, NV, SQ, RS, OG) , including the 2D diagonal edge *DE* and the 0D neural vertex *NV*, and their prisms (DP, AE, SP, RP, OP) , which include the $\sqrt{2}$ diagonal prism and the regular prism *OP*.

In reverse order of classes, the 10 distinct Class III $\{2,3,4|2,3,4\}$ honeycombs may be characterized by the alternation of two *PPs*, each situated at the nodes of a Reference Cubic Lattice (*RCL*), the nodes of one lattice being at the centers of the cubes of the other lattice. In self-reflexive honeycombs, the two *PPs* are the same polytope. In both kinds of honeycomb, *NEs* mediate adjoining or adjacent pairs of *PPs* of the same kind along *XYZ* axes. In the simple lattices, these *NEs* are developed through the expansion sequences into 1D, 2D or 3D polytopes. Figure 1 shows the bicubic 3D schema of the honeycomb order that I have previously advanced [1, 2], in which the two *PPs* are diagonal opposites on either the lower

or upper squares, or are self-reflexive nodes of the upper square. This schema situates the various *GEs* and *PPs* into a coherent order, with each Class III honeycomb represented as a horizontal lower edge, upper diagonal, or vertical (self-reflective) circle of the structure, each Class II honeycomb as a long quadrilateral (diamond) section, and the Class I honeycomb as the diagonals and one pair of opposite edges of the middle square. I describe each of these 10 honeycombs of Class III as a *simple alternation*.

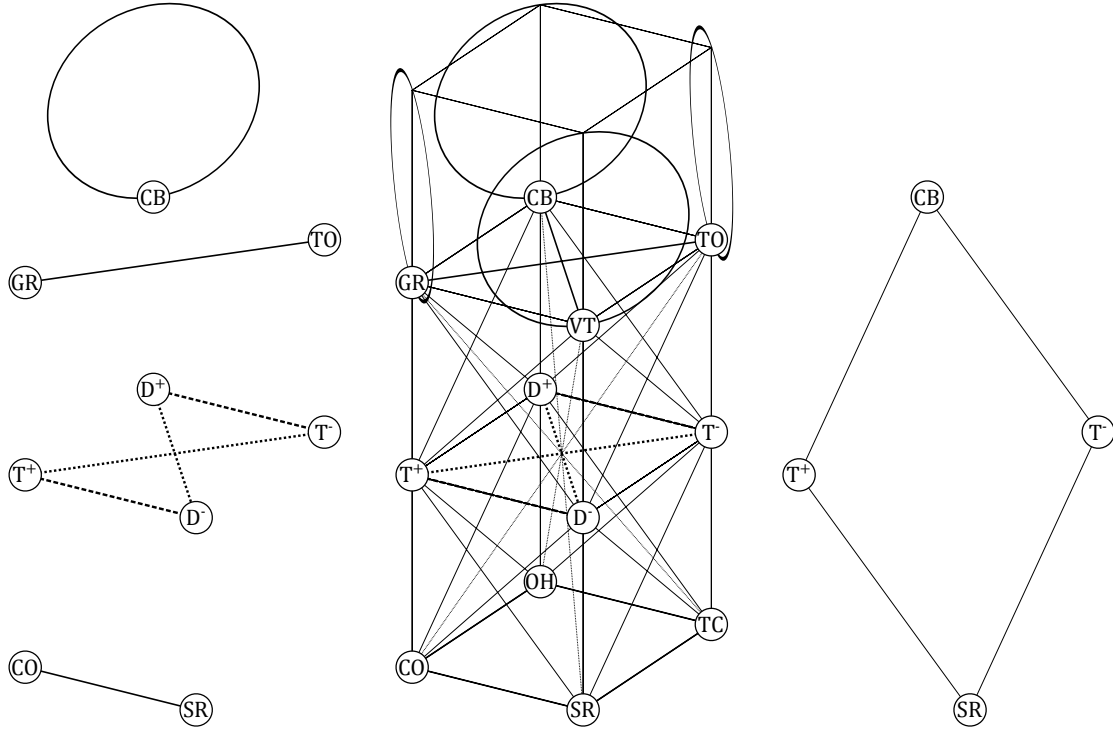


Fig. 1. Bicubic 3D metaorder of the *GEs* and *PPs* with linkages representing the distinct honeycombs.

The singular Class I honeycomb is the middle square with dotted lines (i.e. $D^+ : T^- : T^+ : D^-$, left below); the 4 Class II honeycombs are the four long bicubic sectional diamonds (e.g. $CB : T^+ | T^- : SR$, right); the 6 non-self-reflective Class II honeycombs are the 2 diagonal pairs of the upper square (e.g. $GR : TO$, upper left), and the 4 edge pairs of the lower square (e.g. $CO : SR$, bottom left); and the 4 self-reflective Class II honeycombs ($VT : VT$ is the null case) are the 4 circles at top (e.g. $CB : CB$, top right).

The 4 distinct Class II $\{2,3,3|2,3,4\}$ honeycombs are characterized by the same alternation of polyhedra at nodes of the two *RCLs*; but a further alternation develops of the two sets of tetrahedral nodes of either lattice. One *RCL* alternates nodes of one kind of *GE* of alternating orientation, +ve and -ve, so $RCL_1 = GE_\alpha^+ + GE_\alpha^-$ or $RCL_1 = GE_\beta^+ + GE_\beta^-$, while the other *RCL* alternates nodes of different *PPs*: $RCL_2 = PP_1 + PP_2$. *NEs* are of 0D, 1D or 2D, and do not develop into 3D. In my key 3D schema (Fig. 1) [2], the *GEs* are located in the central

square, while the two different *PPs* are at opposite nodes of the long diagonals of the schema. I describe each of these 4 honeycombs of Class II as an *alternation of alternations*.

The distinct Class I $\{2,3,3|2,3,3\}$ honeycomb is characterized by a more complex alternation pattern, where one *RCL* alternates tetrahedral sets of T^+ and D^- , whilst the other *RCL* alternates tetrahedral sets of D^+ and T^- : $RCL_1 = T_\alpha^+ + D_\beta^-$, and $RCL_2 = D_\alpha^+ + T_\beta^-$. Thus I describe the singular honeycomb of Class I as a *true 4-way/fold alternation*.

I recognize $10 + 4 + 1 = 15$ distinct honeycombs in all, though one is of zero dimension. The 16 honeycombs of Class III show several equivalent honeycombs ($TO|GR, GR|TO$; $ST|TC, TC|SR$; $OH|TC, TC|OH$; $SR|CO, CO|SR$; $OH|CO, CO|OH$; and $VT|CB, CB|VT$; and thus reduce to 10 distinctive arrays. I recognize the Vertex (*VT*) as a *PP*; and in consequence, recognize a seed honeycomb $VT_1|VT_2$ that consists of coincident VT_1 's and VT_2 's in a single point. I differentiate the Cubic honeycomb into three forms (i.e., two distinct honeycombs): the two equivalent honeycombs $VT_1|CB_2$ and $CB_1|VT_2$; and the self-reflective $CB_1|CB_2$.

2. Expansion Sequences of the Regular Honeycombs

The $\{2,3,4|2,3,4\}$ and $\{2,3,3|2,3,4\}$ honeycombs may then be characterized into expansion sequences, in which at each step, the lattice cell length increases by unit length of the component polyhedra. Of critical note, these sequences may be used to formally interrelate the honeycombs into a meaningful metaorder; i.e., they appear to be important organizational features of the metaorder of honeycombs. The $\{2,3,4|2,3,4\}$ honeycombs may thereby be differentiated into one Primary, two Secondary, and one Tertiary sequences, each of two steps, i.e. 1. Contracted \rightarrow Intermediate, and 2. Intermediate \rightarrow Expanded. Figure 2 shows that in the first step, the initial Contracted honeycomb can expand in two different ways, into two different Intermediate honeycombs of the same lattice size, depending on which set of *PPs* separates, and which set of *PPs* morphs. In the second step, the complementary process of separation and morphing occurs, so that both pathways culminate in the same final Expanded honeycomb. These dual pathways of expansion form clusters of sequences that provide a coherent order for the class; and there are also cross-class similarities that I later address.

In the Primary and Tertiary sequences of Class III, the two Intermediate honeycombs are simply alternative cases of the same honeycomb, depending on which *PP* is associated with which *RCL*, so are what I term equivalent honeycombs. In the Secondary sequences, the two Intermediate honeycombs are distinct forms, but one sequence cluster is simply the alternative case of the other, again depending on which *PP* is associated with which *RCL*; one Secondary sequence cluster is thus the mirror reflection of the other.

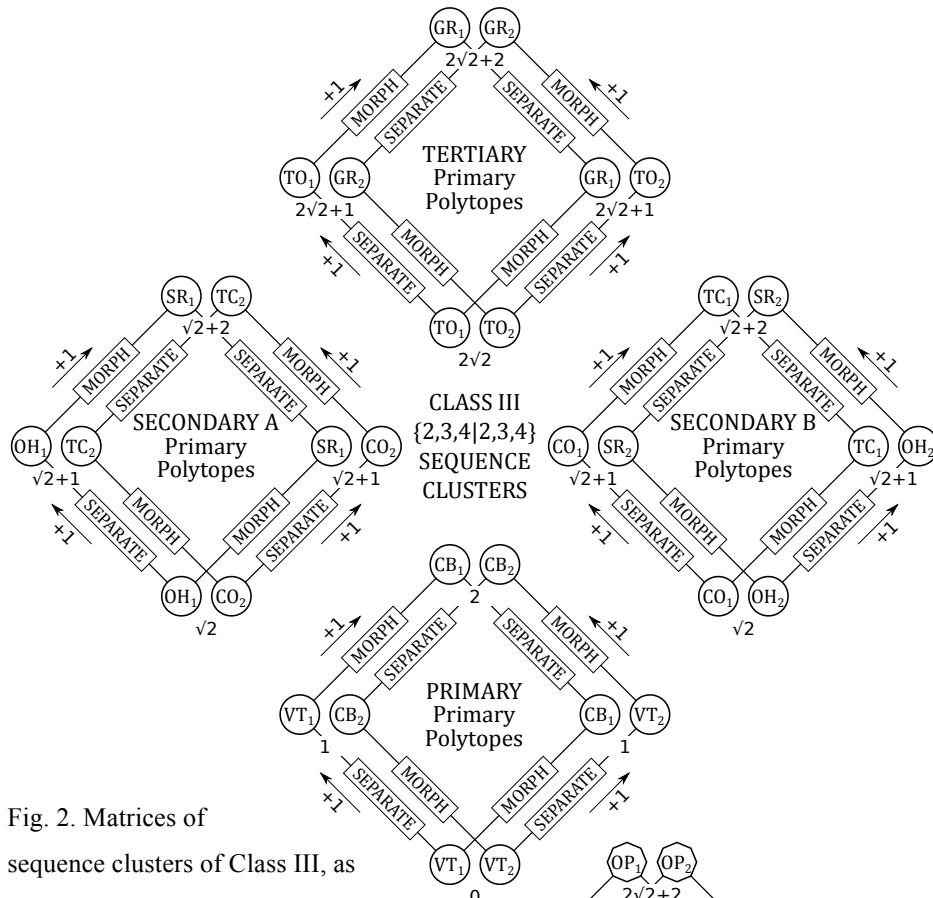
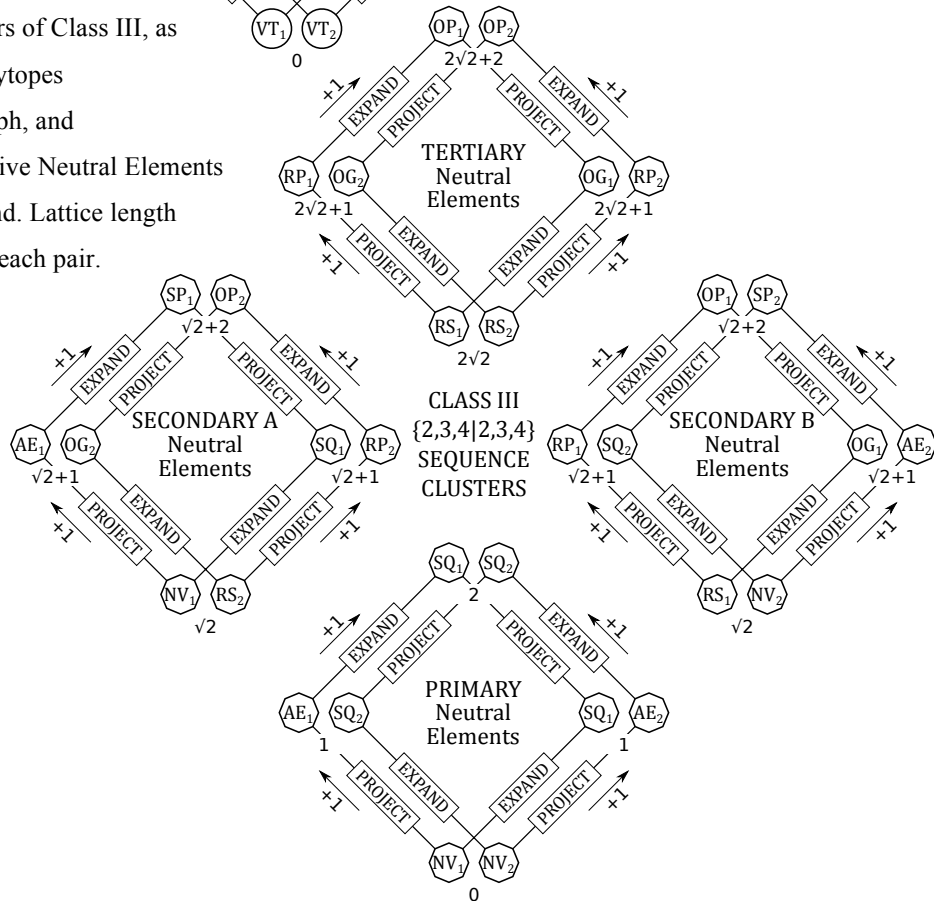


Fig. 2. Matrices of sequence clusters of Class III, as (a) Primary Polytopes separate or morph, and (b) their respective Neutral Elements project or expand. Lattice length is shown under each pair.



2.1. Simplified Description of the Expansion Sequences

I now consider the specific expansion sequences of the regular honeycombs. These are the 2-step sequences of the $\{2,3,4|2,3,4\}$ honeycombs, in which 3D neutral polyhedra might arise; and the 1-step sequences of the $\{2,3,3|2,3,4\}$ honeycombs, in which 3D *NEs* do not arise. In each case, expansion occurs by the unit length of the polyhedra of the honeycomb.

Type 1 and 2 expansion sequences are easiest understood by examining the case of the $CO|OH \rightarrow CO|SR / TC|OH \rightarrow TC|SR$ sequence. Space only permits simple coverage here.

The typical Type 1 $\{2,3,4|2,3,4\}$ expansion sequence commences at the most contracted form of two sets of polyhedra, in this case, *CO* and *OH*. There are two paths the expansion can take to reach the same full expansion. In either pathway, in the *first* step, one set of *PPs*, which are initially in contact, *separate* from one another, so that adjoining *PPs* reach a limit of unit distance from one another. They retain their relative orientations to one another, and remain coaxial on the *XYZ* axes; the lattice has expanded by 1 unit distance, without the *PPs* changing size. Meanwhile as this lattice expands, the other set of *PPs* simultaneously *morph* into a different set of *PPs*. So in this particular case, as the *OHs* of the $[CO|OH]$ honeycomb separate from one another in a regular decentralized expansion, the other primary *COs* morph into *TCs*, to achieve the $[TC|OH]$ honeycomb. In the *second* step, the *PPs* that morphed in the first step are retained, but now *separate* from one another; meanwhile the *PPs* that remained in the first step expansion now simultaneously *morph* into a different *PP*. So in this example sequence, the primary *TCs* now *separate* from one another by unit distance, creating neutral *OPs* between them; meanwhile the other primary *OHs* simultaneously *morph* into *SRs*, creating neutral *SPs* between them.

But this is just one of the two paths that the two-step expansion from $[CO|OH]$ to $[TC|SR]$ can take. In the other path, in the *first* step, the *other* primary set of *COs* *separate* from one another in a regular decentralized expansion, creating neutral *RPs* between them; meanwhile the *remaining* primary set of *OHs* simultaneously *morph* into primary *SRs*, to achieve the $[CO|SR]$ honeycomb. In the second step, the *PPs* that morphed in the first step are retained, but now *separate* from one another; meanwhile the *PPs* that remained in the first-step expansion simultaneously *morph* into different *PPs*. So here, primary *SRs* now *separate* from one another by unit difference, creating neutral *CBs* between them; meanwhile primary *COs* simultaneously *morph* into primary *TCs*, creating neutral *OPs* between them, to end in the $[TC|SR]$ honeycomb. The morphs are $OH \rightarrow SR$ and $CO \rightarrow TC$.

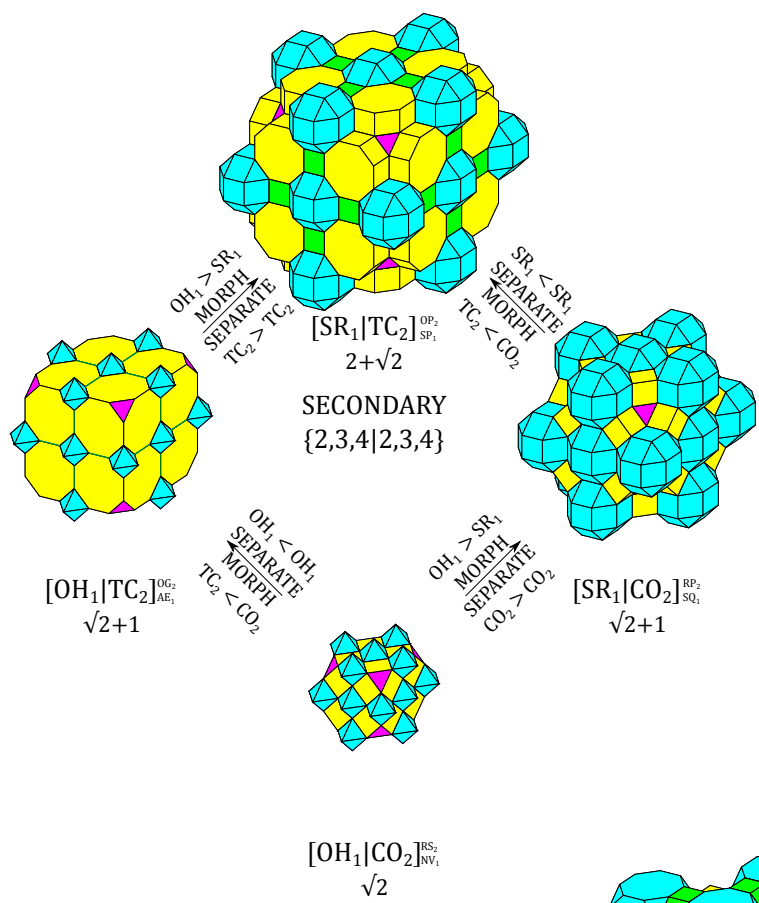
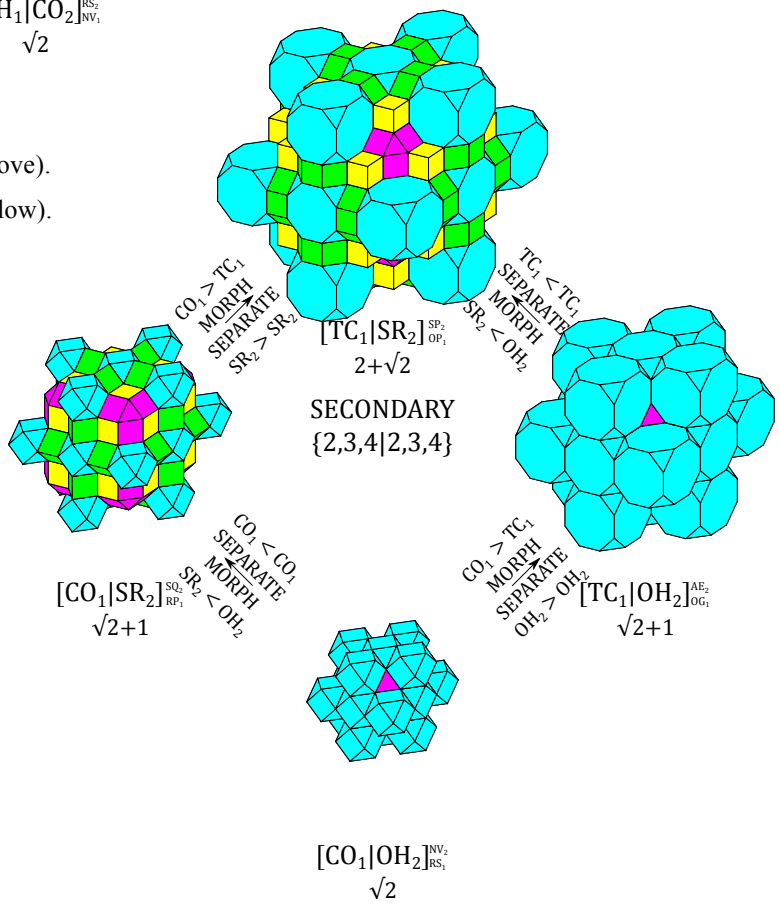


Fig. 3. Clusters of Class III

(a) Secondary A sequences (above).

(b) Secondary B sequences (below).



The other Type 1 $\{2,3,4|2,3,4\}$ expansion sequences are firstly what might be regarded as the equivalent honeycomb of that already described, which in practice terms is identical; and secondly the $VT|VT \rightarrow VT|CB / CB|VT \rightarrow CB|CB$ and the $TO|TO \rightarrow TO|GR / GR|TO \rightarrow GR|GR$ sequences, which are easier to follow, as both start from PP pairs that are the same as each other, and both finish in PP pairs that are the same as each other. In addition, the two intermediate honeycombs for each of these sequences may be regarded as equivalent honeycombs of one other, so only one path of the two for each sequence need be considered.

In the primary $VT|VT \rightarrow VT|CB / CB|VT \rightarrow CB|CB$ sequence, both sets of PPs of the most contracted $[VT|VT]$ honeycomb are vertices, and the honeycomb is of zero size; all vertices coincide in the one 0D point (but paradoxically are presumed to have unit length virtual edges). In the first step of the expansion, one primary set of VTs expands, so that (adjacent) VTs assume unit distance from one another. Meanwhile, the other primary set of VTs morph into primary CBs , forming a cubic lattice, whose vertices coincide with the cubic lattice of vertices of the expanded set of VTs .

In the second step of the expansion, the previously morphed primary CBs expand to unit distance from each other, and in the process, neutral SPs form between adjoining pairs of primary CBs . Meanwhile, the other expanded primary VTs simultaneously morph into primary CBs , and in the process, neutral SPs also form between adjoining pairs of (the other) primary CBs . Each subarray of primary CBs and its neutral SPs forms a counterform to the other subarray - the two arrays are identical, and everywhere interpenetrating; but the two subarrays are simply displaced (by $(\pm 1, \pm 1, \pm 1)$) relative to the other.

In the greatest expansion sequence of $TO|TO \rightarrow TO|GR / GR|TO \rightarrow GR GR$, the Contracted form is of two sets of TOs in the $TO|TO$ honeycomb. In the first step, one set of TOs in RS face-to-face contact expands to assume unit distance, so that adjoining pairs of TOs create neutral RPs between each other; meanwhile the set of TOs morphs to become GRs , so that adjoining pairs of GRs create neutral axial OGs between each other, the pairs of GRs being in face-to-face contact. The two primary sets of TOs and GRs form the Intermediate $TO|GR$ honeycomb. In the second step, the previously morphed primary GRs in neutral OG face-to-face contact expand to unit distance apart, while the neutral axial OGs project to form neutral OPs ; meanwhile the other primary set of TOs in neutral RS face-to-face contact morphs into primary GRs , so that pairs of adjoining primary GRs develop neutral OPs between each other, the neutral RSs thus projecting into neutral OPs separating this set

of *GRs*. Both sets of *GRs* and their respective sets of *OPs* together form the expanded $[GR|GR]$ honeycomb.

3. The Behavior of the Neutral Elements in the Expansion Sequences

3.1. Class III Neutral Elements

In this paper, the expansion sequences of Class III honeycombs have been characterized as in the first step, the elements of one set of *PPs* separate from each other, while the elements of the other set morph from one *PP* into a different *PP*; meanwhile in the second step, the converse occurs. In Class III, adjoining or adjacent pairs of *PPs* of one kind along the XYZ axes are mediated by Neutral Elements, *NEs*. In the contracted form, these *PPs* are adjoining, meaning that they share at least a vertex, if not an edge or a face: adjoining pairs of VT_1 's and VT_2 's of $VT|VT$ are thus mediated by neutral vertices NV_1 and NV_2 , respectively; adjoining pairs of OH_1 's and CO_2 's of $OH|CO$ are mediated by neutral NV_1 and RS_2 , respectively; adjoining pairs of CO_1 's and OH_2 's of $CO|OH$ are mediated by neutral RS_1 and NV_2 , respectively; and adjoining pairs of TO_1 's and TO_2 's of $TO|O$ are mediated by neutral RS_1 and RS_2 , respectively. These *NEs* (in Class III) are all considered to be of $\{2,2,4\}$ symmetry, so they have a primary axis that accords with either the X, Y, or Z axis, the other two axes being the remaining Cartesian axes. Separation of one set of *PPs* is always along an X, Y, or Z axis; therefore, it is readily recognized that in this process, the *NE* will be projected into prismatic form. In the first step from the contracted honeycomb to the intermediary honeycomb, NV projects to axial edge AE (this is easy to see in $OH|CO \rightarrow OH|TC$), while rotated square RS projects to rotated cube/prism RP . The intermediary stage introduces the adjoining *PPs* CB , TC , SR , and GR . Hence, SQ *NEs* mediate pairs of adjoining CBs ; OG mediates pairs of adjoining TCs ; SQ mediates pairs of adjoining SRs ; and OG mediates pairs of adjoining GRs , all along XYZ axes. In the second step of the expansion, these project along with their separating *PPs*, so the square mediating adjoining cubes ($CB:SQ:CB$) projects and separates, respectively, to $CB:SP:CB$; $TC:OG:TC$ to $TC:OP:TC$; $SR:SQ:SR$ to $SR:SP:SR$; and $GR:OG:GR$ to $GR:OP:GR$. So $SQ \rightarrow SP$ and $OG \rightarrow OP$. This accounts for all of the *projecting* neutrals in Class III.

However, there are also the *NEs* that mediate or separate adjoining or adjacent pairs of morphing *PPs*. Each *PP* both separates and morphs in turn, so the initial *NE* can be assumed to be as before. In this case, instead of projecting, the *NE expands* as its *PPs* morph. This can

best be understood in the figures, but the separations:expansions:separations (recalling that these are either $PP_1:NE_1:PP_1$ or $PP_2:NE_2:PP_2$, not mixes) are:

$$\begin{aligned} VT:NV:VT &\rightarrow CB:SQ:CB \text{ and } VT:NV:VT \rightarrow CB:SP:CB, \\ OH:NV:OH &\rightarrow SR:SQ:SR \text{ and } OH:AE:OH \rightarrow SR:SP:SR, \\ CO:RS:CO &\rightarrow TC:OG:TC \text{ and } CO:RP:CO \rightarrow TC:OP:TC, \text{ and} \\ TO:RS:TO &\rightarrow GR:OG:GR \text{ and } TO:RP:TO \rightarrow GR:OP:GR. \end{aligned}$$

So each morph of PP to PP' is associated with two expansions of neutral elements, a lower and a higher, so PP morph $VT \rightarrow CB$ is associated with NE expansions $NV \rightarrow SQ$ and $NV \rightarrow SP$; $OH \rightarrow SR$ with $NV \rightarrow SQ$ and $AE \rightarrow SP$; $CO \rightarrow TC$ with $RS \rightarrow OG$ and $RP \rightarrow OP$, and $TO \rightarrow GR$ with $RS \rightarrow OG$ and $RP \rightarrow OP$. This then accounts for all the expanding neutrals in Class III. In summary, the NEs of separating PPs project, while the NEs of morphing PPs expand.

(Note that in this paper, lattice expansion with constant polyhedral edge length is assumed; the complementary perspective would be to consider the lattice dimension as constant, and the edge length of the polyhedra reducing at each expansion step).

3.2. Class II Neutral Elements

The neutral polytopes can also be considered in Class II. During the two expansion sequences, as the GEs separate, the DEs ($\sqrt{2}$ edges) that mediate these GEs of $T^+ + T^-$ and $D^+ + D^-$ in each contracted form, *project* to become DPs (axial rotated squares) in the expanded form, respectively. Meanwhile, in the Primary Sequence, the NVs mediating alternating VTs and OHs along the XYZ axes *expand* to become SQs ; while in the Secondary Sequence, the RSs mediating alternating COs and TOs along the XYZ axes *expand* to become OGs . The rigorous similarities can be observed between the two sequences.

3.3. Class I Neutral Elements

For complete coverage, neutral polytopes in the singular Class I honeycomb (along the $\sqrt{1}$ axes) consist of diagonal edge DEs , so that one set of XYZ axes consist of strings of $D^+:DE^\backslash:T^-:DE^\prime:D^+:DE^\backslash:T^-:DE^\prime:D^+ \dots$, while the other set of XYZ axes consist of strings of $D^-:DE^\prime:T^+:DE^\backslash:D^-:DE^\prime:T^+:DE^\backslash:D^- \dots$ (where DE^\backslash and DE^\prime for a given XYZ axis are at right angles). NEs of $HG:TR^+:V3:TR^-:HG \dots$ also develop along the $\sqrt{3}$ axes, but in this paper, I do not consider the $\sqrt{2}$ or $\sqrt{3}$ relationships of NEs in detail. This class, having just one distinct form, does not develop sequences.

4. The Four Key morphs that Characterize the Various Expansion Sequences

4.1. The Key Morphs in Class III

Inspection of the Class III four-fold clusters of four-fold honeycombs and their sequences reveals the elegant regularity of the separations and morphs of the PPs across the entire class. Each separation of a PP occurs just twice, so predictably there are 8 kinds of separations: ($VT \rightarrow VT$, $CB \rightarrow CB$, $OH \rightarrow OH$, $CO \rightarrow CO$, $TC \rightarrow TC$, $SR \rightarrow SR$, $TO \rightarrow TO$, $GR \rightarrow GR$). Each morph of a PP into another PP occurs four times, so there are just 4 kinds of morphs: $VT \rightarrow CB$, $OH \rightarrow SR$, $CO \rightarrow TC$, $TO \rightarrow GR$. Morph pairs are uniquely determined by their PPs having common polytopes as ‘faces’ on their $\sqrt{3}$ axes: $V3$ for VT, CB ; TR^+ for OH, SR ; TR^- for CO, TC , and HG for TO, GR . So in a certain sense, each morph could be regarded as the respective $\sqrt{3}$ axis faces separating away from each other by unit distance along the XYZ axes, as one contracted polyhedron becomes its expanded morph.

4.2. The Key Morphs in Class II

Inspection of the Class II two-fold clusters of two-fold honeycombs and their sequences reveals further elegant regularity of the separations of the GEs and the morphs of the PPs across that entire class. In this case, each separation of a GE occurs just once, there thus being four kinds of separation, but these now occur in pairs, so ($T^+ \rightarrow T^+$ and $T^- \rightarrow T^-$), and ($D^+ \rightarrow D^+$ and $D^- \rightarrow D^-$). Meanwhile, the same four morphs occur; each morph occurs just once, but these also appear in pairs, so ($VT \rightarrow CB$ and $OH \rightarrow SR$), and ($CO \rightarrow TC$ and $TO \rightarrow GR$). This represents a natural pairing of morphs that occurs. At the same time, there is a natural pairing of PPs according to their $\sqrt{1}$ faces, so each pair has the same $\sqrt{1}$ face. The behavior of the NEs is described in the penultimate paragraph of the preceding section.

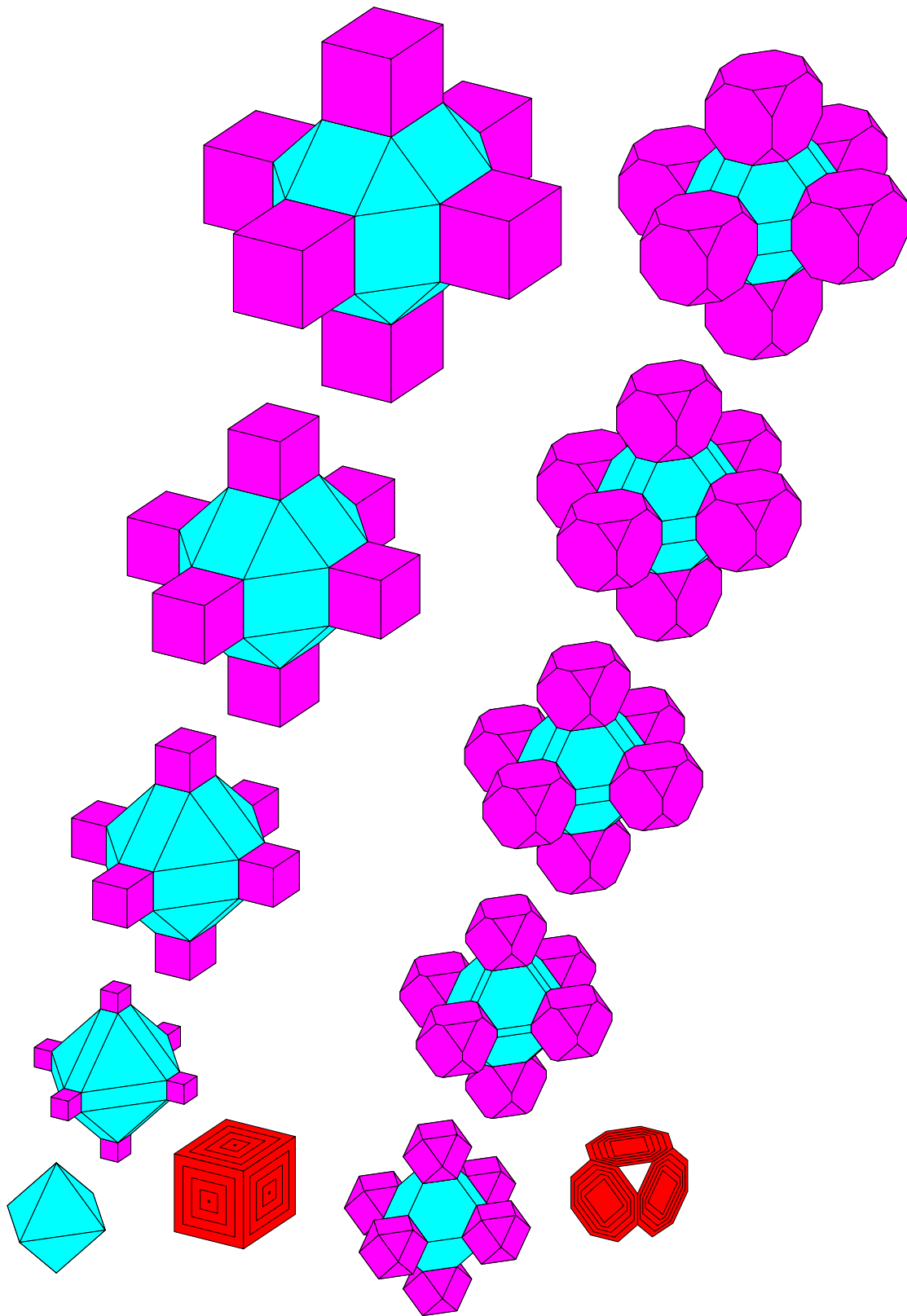


Fig. 4. $OH \rightarrow SR$ and $VT \rightarrow CB$, and $TO \rightarrow GR$ and $CO \rightarrow TC$ Morphs of Class II, with progressions of their NEs. (In Class III, there is just one of these morphs per sequence step).

5. Extension of the Order to include the {2,3,6} and {2,4,4} Tessellations of the Plane

One of the genuine delights of research is the recognition of the validity of the postulates made when they suggest extensions to related behavior and structure, and when the predictions they allow are then confirmed through inspection and experimental investigation. This occurred in my initial seminal paper on the metaorder of the regular and semi-regular polyhedra [4] (considered as individual entities, not honeycombs), when the common formal structure for the 3D symmetries of {2,3,3}, {2,3,4}, and {2,3,5} firstly suggested equivalent snub forms each class, which enabled me to generalize the {2,3,3} jitterbug system of R. Buckminster Fuller into the equivalent {2,3,4} and {2,3,5} jitterbug systems; and secondly in the generalization of that 3D metaorder of polyhedra to rigorously account for the regular and semi-regular 2D tessellations of the plane, via the {2,3,6} and {2,4,4} symmetry classes (together with their corresponding 2D jitterbug systems via the corresponding skew forms).

Here, I came to realize that the 3D honeycombs would likely be analogued in 2D by the tessellations of the plane. And indeed, I have been able to generalize the component diamonds of my Class III sequence clusters, with alternating successions of separation and expansion, to rigorously classify the two classes of the regular and semiregular tessellations of the plane, of {2,3,6} and {2,4,4} symmetry, respectively. Rather than exhaustively describe these, which space here does not permit, I simply illustrate their respective formal orders (Figs. 5 & 6).

6. Extension of the honeycomb order to revision of the original metaorder of regular and semiregular polyhedra and tessellations of the plane

The experimental investigation into the extension of the order to the 2D tessellations, and its clear validity, in turn led to reinvestigation of my original order of the regular and semiregular 3D polyhedra (and 2D tessellations). The initial impetus was the recognition of the virtual *VT* as a *PP*, which suggested that it should be integrated into the metaorder, at least for the {2,3,4} symmetry class. Clearly, the *VT PP* belonged along the main vertical axis, and fitted below the horizontal truncation axis. I then mapped the four honeycomb morphs and the pairs of Class II honeycomb *PPs* onto my original metaorder. Although the pairs precisely mirrored the morphs, I was frustrated by the apparent irregularity this presented between the two sequence clusters involved; they were clearly parallel, and should have the same form. I was able to resolve this by restructuring the two-axis structure of the original metaorder into two overlaid diamonds (Fig. 7), thus describing a fundamental differentiation of the now 8 {2,3,4} *PPs* into two parallel sets of 4, a lower, and an upper set, (the only drawback being that the horizontal truncation sequence $OH \leftrightarrow TO \leftrightarrow CO \leftrightarrow TC \leftrightarrow CB$ now becomes an “M” shape).

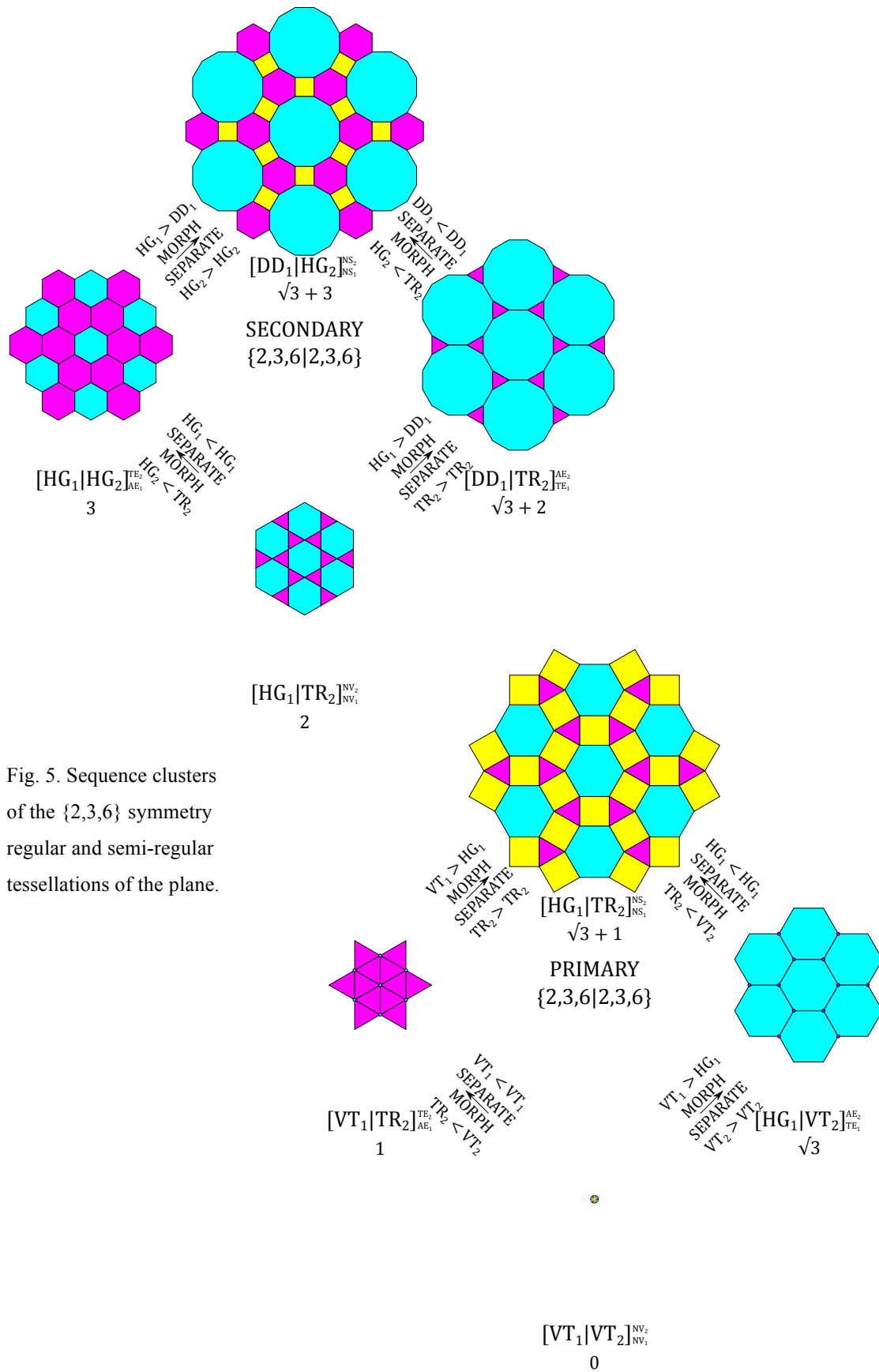


Fig. 5. Sequence clusters of the $\{2,3,6\}$ symmetry regular and semi-regular tessellations of the plane.

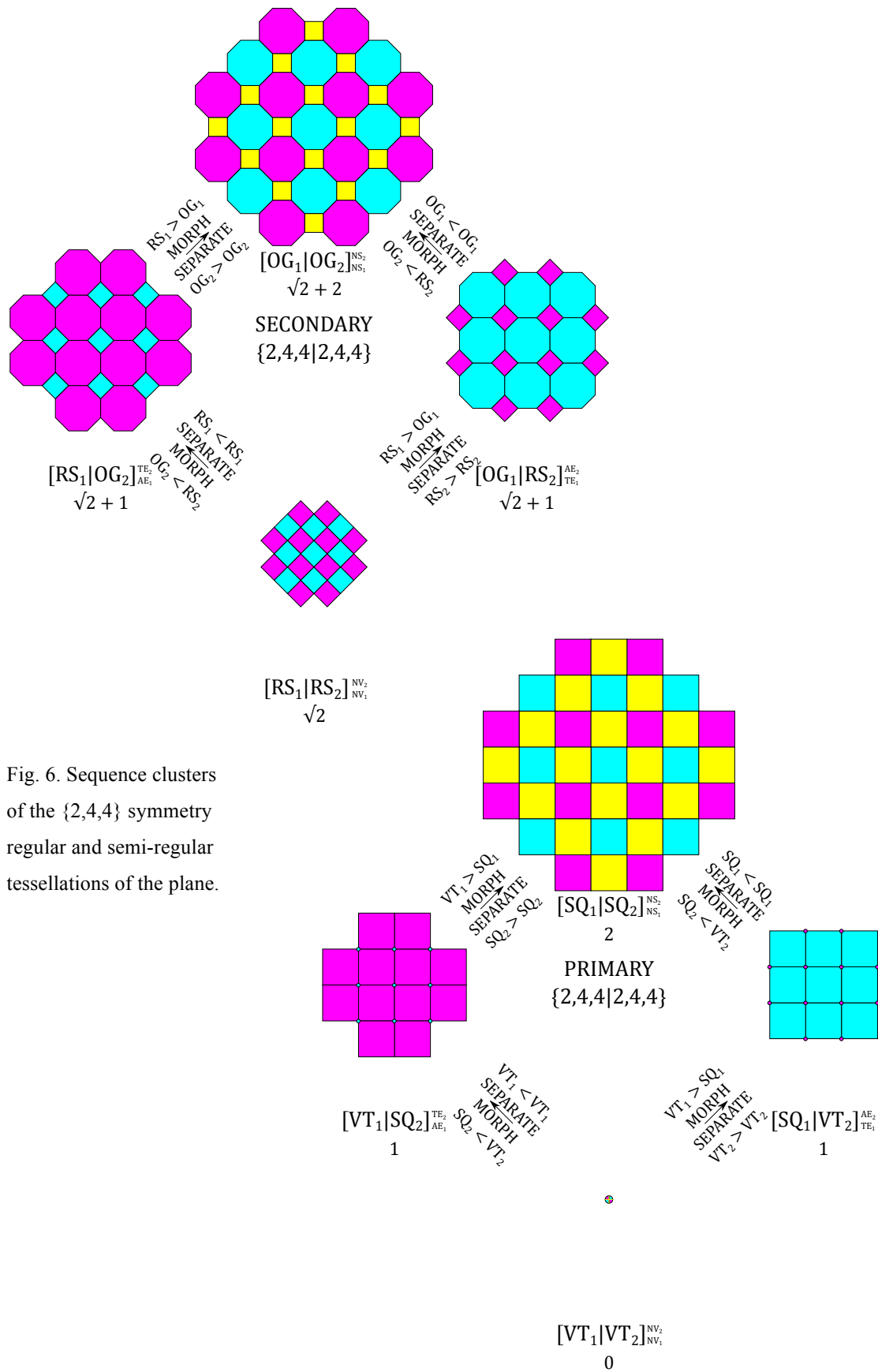


Fig. 6. Sequence clusters of the $\{2,4,4\}$ symmetry regular and semi-regular tessellations of the plane.

In future research, I will describe this revision of my formal metaorder of the regular and semiregular polyhedra and tessellations in detail, as it is critical to a proper understanding of these polytopes, and a metaorder that carries through to the metaorder of the honeycombs.

7. Conclusion

The transformational geometry of these honeycomb sequences offer potential for real-world structures and behavior, e.g., nanoscale engineering (new materials, micro-architected materials [5], metamaterials), transfer interfaces (tissue engineering, battery electrodes, filters), environmental response (solar cells, sensors), kinetic architectural and engineering structures (space frames), and dynamic structures in microgravity for deployment in Space (antennae, space habitations and stations). I hope to address this potential in future research, after first more fully elucidating the sequences, sequence clusters, and the integral properties of the key polyhedral honeycombs. Proper understanding of the spatial order, including the transformations of the expansion sequences, and the remarkable consistency of the patterns that maintain unit edge length and constrained $\sqrt{1}$ and $\sqrt{2}$ orientations to the cardinal XYZ cubic lattice will enable designers to better utilize these beautiful forms, whilst encouraging further research into their coherent integrity of harmonic pattern, which reveals in some measure the extraordinary nature of empirical space.

References

- [1] R. C. Meurant, Towards a Meta-Order of the All-Space-Filling Polyhedral Honeycombs through the Mating of Primary Polyhedra, *Information* 19: 6(B), June 2016, 2111–2124.
- [2] R. C. Meurant, Towards a New Order of the Polyhedral Honeycombs: Part II: Who Dances with Whom?, in L. Li and T.-W. Kuo (eds.), *Proceedings of The Seventh International Conference on Information*, Taipei, (2015), Nov. 25–28, 369–373.
- [3] R. C. Meurant, Sequences of the All Space-filling Periodic Polyhedral Honeycombs, in L. Li et al. (eds.), *Proceedings of The Eighth International Conference on Information*, Tokyo, (2017), May 17–18.
- [4] R. C. Meurant, A New Order in Space - Aspects of a Three-fold Ordering of the Fundamental Symmetries of Empirical Space, as evidenced in the Platonic and Archimedean Polyhedra. *International Journal of Space Structures*, Vol. 6 No.1, University of Surrey, Essex, pp. 11–32 (1991), via <http://rmeurant.com/its/harmony.html>
- [5] S. C. Han, J. W. Lee, K. Kang, A new type of low density material; Shellular, *Adv. Mater.* 27 (2015) 5506–5511.